**Rare Metal Materials and Engineering**
Volume 48, Issue 10, October 2019
Available online at www.rmme.ac.cn

Science Press

**Cite this article as:** Rare Metal Materials and Engineering, 2019, 48(10): 3088-3094.

ARTICLE

# Fabrication of Low-Density Gold with Hierarchical Nanoporous Structure by Templating-Dealloying Synthesis and Its Electrocatalytic Properties

**Chen Jing[1], Lian Lixian[1,2], Liu Ying[1,2], Wang Li[1]**

*[1] School of Materials Science and Engineering, Sichuan University, Chengdu 610065, China; [2] Key Laboratory of Advanced Special Material & Technology, Ministry of Education, Sichuan University, Chengdu 610065, China*

**Abstract:** The composite technique of templating and dealloying was proposed for synthesizing the low-density and hierarchical nanoporous gold (NPG). In this technique, the silica ($SiO_2$) microspheres with an average diameter of ~700 nm were prepared as the sacrificial templates, the Ag@$SiO_2$ and Au@Ag@$SiO_2$ core-shell microspheres were prepared successively via the electroless plating approach, and the Au@Ag@$SiO_2$ alloy bulks were formed through the cold-pressing and sintering method. The results show that by continually changing the corrosion solutions, the templates and the Ag element can be completely eliminated from the Au@Ag@$SiO_2$ alloy. The $SiO_2$ templates are completely removed from Au@Ag@$SiO_2$ microspheres so as to form the large-sized hollow spherical shells (with the diameter of ~675 nm), and the Ag element are eliminated by dealloying so as to generate a lot of small-sized pore (with the diameter of ~75 nm) structures on the shells. TEM images illustrate that the ligaments in NPG consist of the nano-grains with polycrystalline characteristics. The hierarchical NPG foam with low-density of 1.1 g/cm$^3$ (relative density ~5.7%) and high specific surface area of 4.24 m$^2$/g shows excellent catalytic activity and rapid mass transfer rate for methanol electro-oxidation in alkali solution, which implies a promising application in catalysis.

**Key words:** nanoporous gold (NPG); templating and dealloying; hierarchical; low-density; electrocatalytic

Porous metal with extremely low-density is widely used in catalysis, adsorption, sensing, and separation[1-5]. In particular, multimodal or hierarchical porous materials can be used in more specific applications, such as fluidic-based and gas-based facility, because smaller pores result in higher surface area, while the bigger pores guarantee fast and efficient transportation[6]. Hierarchical nanoporous gold (NPG) foams have the characteristics of noble metal, multimodal porous structure and low-density. Thus, they can be well applied in many fields, especially as catalytic electrode materials for direct liquid fuel cell (DLFC). NPG has been demonstrated to have remarkable catalytic activities towards various fuel cell reactions, such as oxidation of methanol[7], ammonia borane[8] and hydrazine[9]. For instance, Zhang reported an NPG fabricated by dealloying an Au-Ag alloy and confirmed that the prepared NPG electrode can be a highly efficient and durable electrocatalyst for methanol[10].

A lot of technologies, such as dealloying[11-14], spark plasma sintering[15], spacer-adding[16-18] and templating[19,20] have been widely used to prepare the porous metal. The dealloying approach is a conventional method for synthesizing nanoporous metal. During the dealloying process, the non-noble components of alloy can be eliminated by the chemical or electrochemical process, and the noble metal atoms can be reformed as the ligament of the nanoporous structure. The template technology is an effective way for fabricating low-density structure or hollow structure. It makes the size and shape of the pores exchangeable and adjustable. According to the literature, the hierarchical porous gold monoliths with density as low as 0.28 g/cm$^3$ can be synthesized by eliminating

---

Received date: October 23, 2018
Foundation item: Chengdu Science and Technology Huimin Project (2015-HM02-00067-SF); Scientific and Technical Project of Sichuan Province (2016GZ0225)

Corresponding author: Lian Lixian, Ph. D., Professor, School of Materials Science and Engineering, Sichuan University, Chengdu 610065, P. R. China, Tel: 0086-28-85405332, E-mail: scu_lianyi@126.com

the template of polystyrene beads (10 and 1 μm in diameter) and dealloying the alloy shells of Ag/Au[12,21]. Thus the combination of template technique and dealloying method not only affords a good way for preparing the hierarchical nanoporous materials, but also proposes an effective way for reducing the density.

In this paper, the combination of templating and dealloying techniques were proposed for synthesizing the NPG foams with low-density, high specific surface area, and hierarchical nano-sized pores. In this synthesis scheme, shown in Fig.1, the monodispersed $SiO_2$ microspheres were chosen as templates and the core-shell Au@Ag@$SiO_2$ microspheres were prepared by electroless plating. Hierarchical NPG foams with low-density were successfully processed by eliminating the templates and dealloying the Au-Ag alloys. Meanwhile, the formation of hierarchical pores and the polycrystalline characteristics of the ligaments were analyzed in detail. At last, to assess the application prospects of the synthesized gold foams in catalysis, the density and the surface area were measured, and the catalytic performance of methanol oxidation was tested.

## 1 Experiment

The schematic illustration of the templating and dealloying technology for synthesizing the hierarchical NPG foams was presented in Fig.1. There are three key steps in the preparation process, including the preparation of Ag@$SiO_2$ microspheres, the preparation of Au@Ag@$SiO_2$ microspheres, and the preparation of NPG foams.

### 1.1 Preparation of Ag@$SiO_2$ microspheres

$SiO_2$ templates were firstly prepared according to the famous Stöber[22] process. Then, templates were functionalized with $Sn^{2+}$ by magnetic stirring in the stannous chloride solution (0.066 mol/L) for about 30 min. Afterwards, these $SiO_2$ templates were activated again by magnetic stirring for 30 min in the silver ammonia solution (0.029 mol/L). Silver plating liquid was achieved by dropping sodium hydroxide (0.125 mol/L) into silver ammonia solution (0.059 mol/L) until the solution was clarified. The reducing agent was a mixed solution of glucose (0.044 mol/L) and sodium potassium tartrate (0.053 mol/L). To plate Ag on the surface of $SiO_2$ templates, the activated microspheres and the silver plating liquid were magnetically stirred for about 2 h, while the reducing agent was added into the mixed solution at the speed of 0.07 mL/s. Finally, prepared Ag@$SiO_2$ microspheres were separated from the mixture by a centrifuge, washed by deionized water, and dried in an oven at 40 ºC for 24 h.

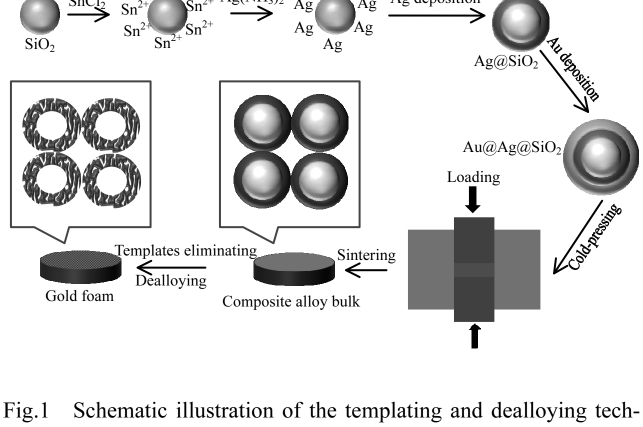

Fig.1 Schematic illustration of the templating and dealloying technique for synthesizing the hierarchical NPG foams

### 1.2 Preparation of Au@Ag@$SiO_2$ microspheres

Gold plating liquid was a mixed aqueous solution of $HAuCl_4$ (0.014 mol/L) and $Na_2CO_3$ (0.315 mol/L). Before plating Au on the surface of Ag@$SiO_2$ microspheres, 0.2 g Ag@$SiO_2$ microspheres were dispersed in 20 mL alcohol with the help of PVP (0.03 g). The reducing agent was diluted with the methanol aqueous solution (10 vol%). Then, the dispersed microspheres and the gold plating liquid were magnetically stirred for about 2 h, and at the same time, the methanol solution was added into the mixed solution at the speed of 0.017 mL/s. Finally, prepared Au@Ag@$SiO_2$ microspheres were separated from the mixture by the centrifuge, washed by deionized water, and dried in the oven at 40 ºC for 24 h.

### 1.3 Preparation of NPG foams

Au@Ag@$SiO_2$ microspheres (0.3 g) were cold-pressed in a stainless steel mold under the pressure of 75 MPa to fabricate bulk composites. Then, bulk composites were heated at 500 °C for 1 h in the tube furnace (under an argon atmosphere) to fabricate alloy bulks. The Au@Ag@$SiO_2$ alloy bulks were alternately and recurrently immersed into the nitric acid and hydrofluoric acid solution to dealloy and remove the $SiO_2$ templates, and its exchange period is 2 d. In the process of corrosion, the concentration of nitric acid gradually increased from 0.28 mol/L to 1 mol/L, and the concentration of hydrofluoric acid increased from 0.45 mol/L to 1 mol/L. After etched for about 30 d, the NPG foams were immersed into the concentrated nitric acid and hydrofluoric acid for about half a day, and then washed by deionized water and ethyl alcohol for several times. At last, prepared NPG foams were dried in the $CO_2$ gas for the subsequent characterization.

### 1.4 Characterization

The phase composition of core-shell microspheres was identified by the X-ray diffractometer (XRD, DX-2000) with Cu Kα radiation. The morphology and microstructure of the samples were characterized by the field-emission scanning electron microscope (FESEM, XL30SFEG) with an X-ray energy dispersive spectrometer (EDS) for elemental analysis. Crystal characteristics of the ligament in the final NPG foam were characterized by the transmission electron microscope (TEM, Tecnai G2 F20 S-TWIN). The automatic surface area and pore size analyzer (Autosorb-1) was used to test $N_2$ adsorption-desorption isotherms and BET surface area of the NPG foams. And the image analysis software (Image-Pro Plus) was used to calculate the size of the plated Au/Ag nanoparticles and the dimension of the ligaments and pores of the NPG foams. All the statistical sizes calculated by Image-Pro Plus were averages.

### 1.5 Electrochemical measurements

Electrochemical tests were carried out at room temperature in a typical three-electrode system connected to an electrochemical workstation (CHI660E, ChenHua, Shanghai). Mercuric oxide electrode (Hg/HgO, 1 mol/L $OH^-$) and Pt electrode were used as reference electrode and counter electrode, respectively, and the prepared NPG samples were used as working electrodes. The final prepared NPG samples were gently ground into powders in an agate mortar. 2 mg powders were picked and spread onto a gold disk electrode, whose head was muffled with a conducting resin. The geometric area of NPG powder, exposed to the electrolyte, was 3.14 $mm^2$. The solution for methanol oxidation was freshly prepared by dissolving methanol in 500 mL 1 mol/L KOH aqueous solutions, and then purged with argon to remove oxygen for about 30 min. The scan rate of cyclic voltammetry (CV) curve was 20 mV/s.

## 2 Results and Discussion

The SEM images of the microspheres in different plated stages and the EDS spectrum of the final plated microspheres are illustrated in Fig.2. As shown in Fig.2a, the $SiO_2$ microspheres with an average diameter of about 700 nm, prepared by a sol-gel method, have good properties of dispersion and uniformity. Fig.2b and 2c show the morphology of the $SiO_2$ microspheres after plating Ag and Ag-Au, respectively. After the processes of sensitizing and activating, the plated Ag shells and Ag-Au shells can enfold the silica microspheres closely and homogeneously. The dimensions of Ag and Ag-Au shells are about 30 and 50 nm, respectively, calculated by the Image Pro Plus software. The appearance of Ag shells and Ag-Au shells is slightly different. Ag shells are composed of many particles, among which there are many spaces. After plating Au onto the Ag shells, shown in Fig.2c, the space among Ag particles gradually becomes smaller and some new cracks appear on the shell. It can be inferred that the newly reduced Au atoms preferentially accumulate in the valley of the Ag particles and form an integrated shell. The cracks might be caused by the abscission of Ag during the rapid stirring process. According to the EDS spectrum (Fig.2d), the final plated shells are composed of Ag and Au with an atomic ratio of 1:1.

Fig.3 shows the XRD patterns of three kinds of microspheres prepared in different plating stages. Obviously, the broad peak of $SiO_2$ reveals the amorphous characteristic of $SiO_2$. The sharp peaks of Ag@$SiO_2$ and Au@Ag@$SiO_2$ well illustrate the crystal form of the grown Ag and Au particles. As Au and Ag have the same face-centered cubic crystal structure and similar lattice constants (0.409 nm versus 0.408 nm), the characteristic peaks of Au and Ag are almost overlapping in Au@Ag@$SiO_2$. Four sharp peaks of Ag@$SiO_2$ and Au@Ag@$SiO_2$ are located at 38.2°, 44.3°, 64.7° and 77.5°, corresponding to the lattice planes (111), (200), (220) and (311), respectively. Above result is in accordance with Ref. [23].

Fig.4 shows SEM images of NPG foams at different stages of dealloying process. Obviously, after 20 d of dealloying, the

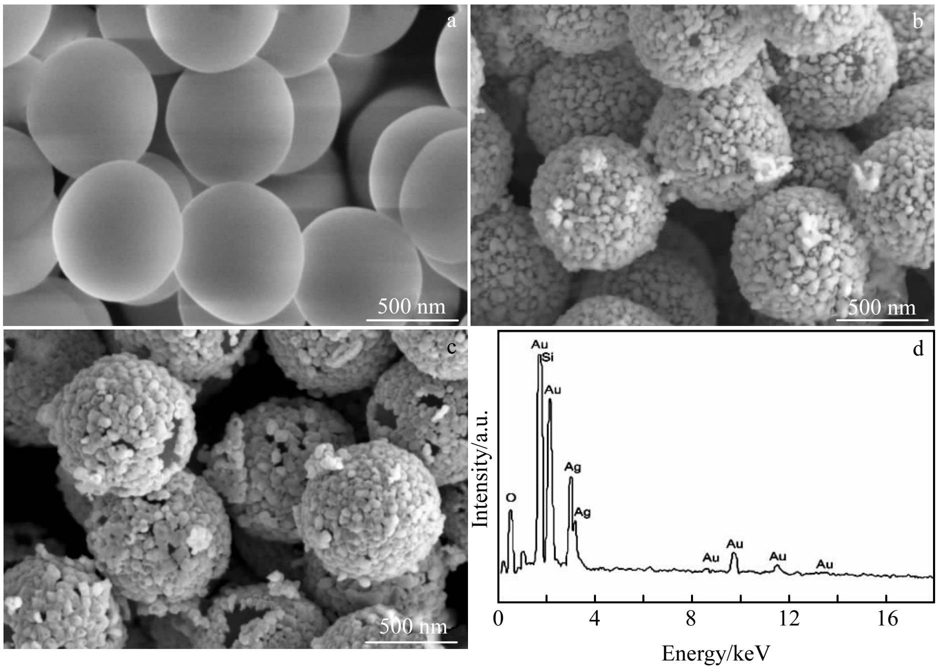

Fig.2 SEM images of the prepared core-shell microspheres: (a) $SiO_2$, (b) Ag@$SiO_2$, and (c) Au@Ag@$SiO_2$; (d) EDS spectrum of Au@Ag@$SiO_2$ microspheres

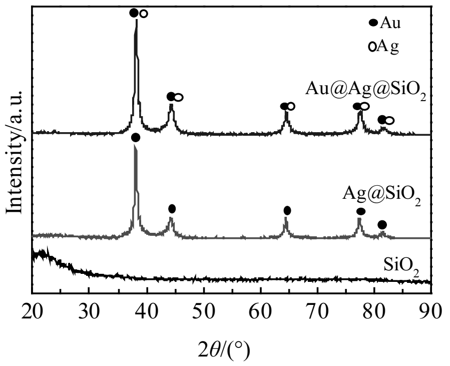

Fig.3 XRD patterns of three kinds of microspheres prepared in different stages of plating

$SiO_2$ particles are completely eliminated. A lot of large-pores (~675 nm in diameter) remain in situ in almost the same scale with the original templates, as shown in Fig.4a. However, the size of pores is a little smaller than that of templates, indicating slight volume shrinkage during etching and drying. Still, the process provides a good control scheme for the size of the pores. Fig.4c, magnified from Fig.4a, shows one hollow shell generated by etching the template. The shell is decorated by a few nano-pores, which may be caused by the preliminary dealloying of the Au-Ag alloy shell. When the etching time increases from 20 d to 30 d, as more Ag elements dissolve, the residual gold atoms tend to self-organize into an interconnected network, composed of the pores and ligaments, on the hollow shell, as shown in Fig.4b and 4d. It can be easily observed that more nano-pores are widespread on the shell when the dealloying time is extended to 30 h. The nano-pores are mainly distributed between 35~100 nm, with an average size of 75 nm, as shown in the inset of Fig.4d. A small number of pores larger than 100 nm may be caused by cracking of the shell during dealloying. The slight deformation cannot be avoided because the ligament is too fine to bear any stress caused by dealloying and drying process. The volume shrinkage ratio in the process is about 16%. The representative SEM images, shown in Fig.4, demonstrate that the prepared NPG foams are composed of large-sized hollow spherical shells (~675 nm in diameter) with some small-sized ligament-pores (~75 nm) distributed on the shells. No cracks occur in the bulk NPG foam, indicating that it is an integrated structure, as shown in the inset of Fig.4b.

In the process of dealloying, the decrease of the Ag content can be demonstrated by the EDS spectra in Fig.4e and 4f. The Ag content of the plating layer is ~50 at% (Fig.2d), which is reduced to ~45 at% (Fig.4e) after 20 d of dealloying and to 2.5 at% after 30 d of dealloying (Fig.4f). The residual Ag content after 30 d of dealloying agrees with the minimum value (about 2 at%) reported in Ref.[24]. At the later stage of etching, the content of Ag is reduced much faster than at the earlier stage. It may be caused by the synthetic action, such as the increase in concentration of nitric acid, and the larger remained cores by the removal of $SiO_2$ particles. As the concentration of nitric acid increases, more $NO_3^-$ is available to be activated by the Ag element. And the larger pores can afford good channels for exchanging the ions in solution. Therefore, the combination of dealloying and templating technology can afford good control

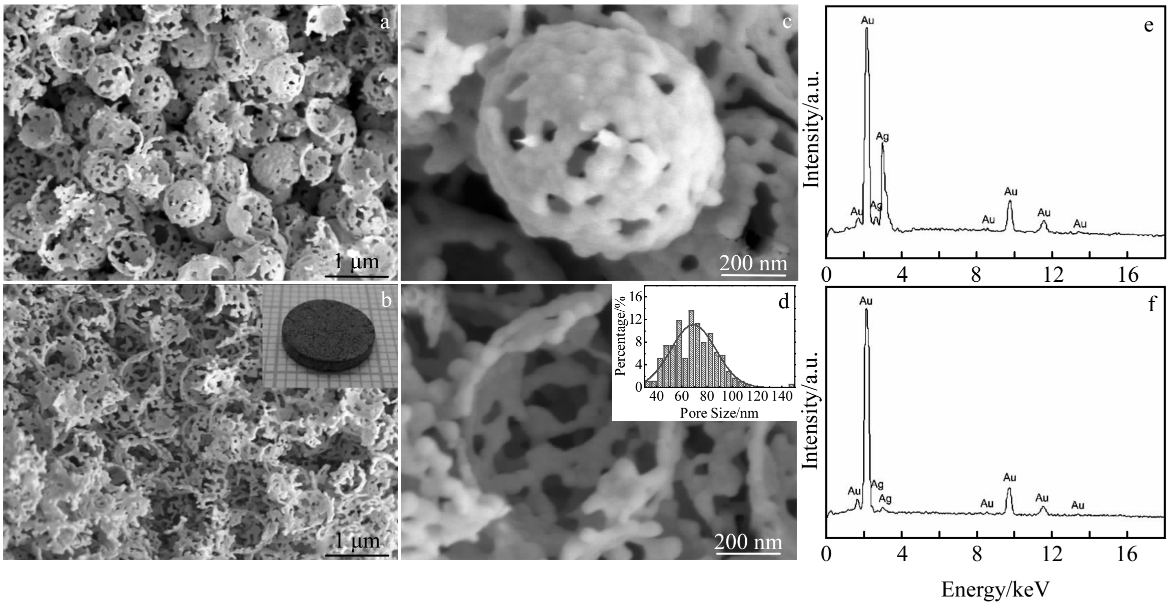

Fig.4 SEM micrographs (a~d) and EDS (e, f) spectra of NPG foams with different dealloying time: (a, c, e) 20 d and (b, d, f) 30 d (inset in Fig.4b is digital image of a final NPG foam, and inset in Fig.4d is pore size distribution of nano-pores)

ability to prepare the gold foams with high surface area, low-density, and fine morphology.

From the TEM images in Fig.5a, the dark skeleton demonstrates the formation of the three-dimensional bi-continuous nanoporous structure, which is in conformity with the SEM images. The average ligament size calculated by Image Pro Plus is about 77 nm. Fig.5b provides a typical high-resolution TEM image of one grain on the ligament of NPG. The highly ordered lattice fringes can be observed in Fig.5b, and its lattice spacing is about 0.23 nm, similar to the (111) *d*-spacing of Au (0.2355 nm) [25]. The inset in Fig.5b provides selected-area electron diffraction (SAED) pattern of one crystalline grain, which exhibits the lattice planes of fcc Au. From Fig.5c, the ligament of the as-prepared NPG consists of many single-crystalline grains with an average diameter of ~42 nm. Above characteristics demonstrate that the gold atoms are self-organized and grow into crystal grains in a certain orientation when the Ag component is dissolved during the process of dealloying. These crystal particles are connected with each other in a random orientation and finally form the ligaments.

The diameter, height, and weight of the final NPG foam were measured in this experiment. The density of the final hierarchical NPG foam, calculated through dividing the mass by volume, is as low as 1.1 g/cm$^3$ (~5.7% of relative density). Fig.6 is the $N_2$ adsorption-desorption isotherm of the prepared bulk NPG foam. It displays type IV isotherms according to the IUPAC classification [26], indicating that most pores belong to mesopores. It should be pointed out that the nano-pores only appear on the shells, and their pore volume is relatively small compared to that of large-pores. In addition, the large-pores (~675 nm in diameter) cannot be detected effectively by $N_2$ adsorption-desorption isotherm. So, the hysteresis in the isotherms is not particularly obvious. The specific surface area of prepared bulk Au foam determined by BET surface analysis is about 4.24 m$^2$/g, which is slightly higher than that of NPG foams prepared in other studies[12,19].

Fig.7a shows the CV curves of two kinds of electrodes in 1 mol/L methanol solution (the current density of gold disk electrode is amplified 5 times). Compared with the gold disk electrode, NPG electrode possesses a higher oxidation peak current density. The current density at the potential of 0.3 V is about 7.3 mA·cm$^{-2}$, which is about 29 times higher than that of the gold disk electrode (0.24 mA·cm$^{-2}$). In addition, the onset oxidation potential ($E_{on}$) of the NPG electrode is about –0.08 V, which is 0.22 V negatively offset from that of gold disk electrode (about 0.14 V). The above results indicate that NPG electrode has excellent electrocatalytic activity, which may benefit from the larger surface area of nanoporous structure.

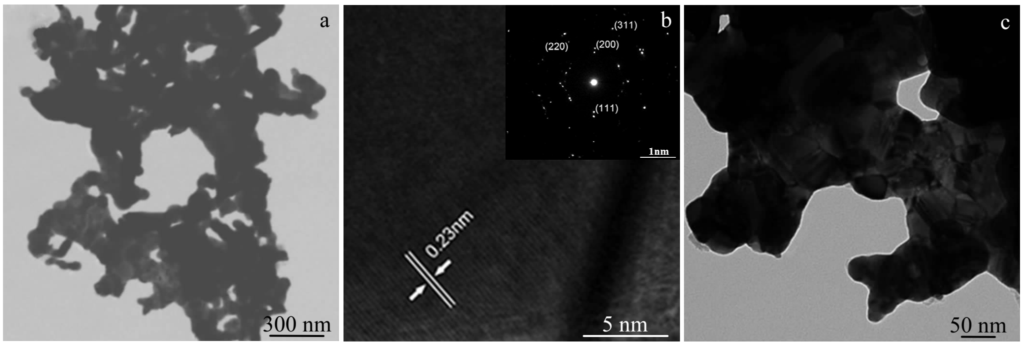

Fig.5 TEM (a, c) and HRTEM (b) images of the final NPG foam (inset in Fig.5b is SAED pattern of the final NPG foam)

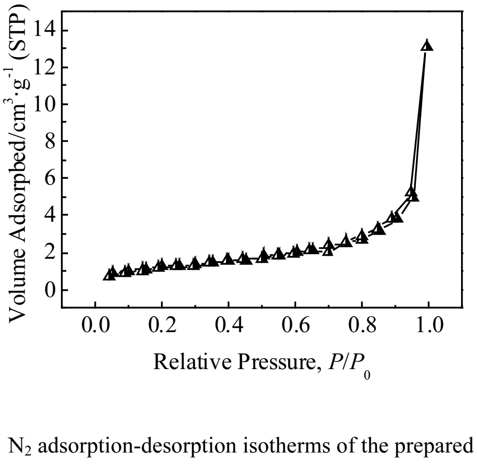

Fig.6 $N_2$ adsorption-desorption isotherms of the prepared bulk Au foam

The CV curves of NPG electrode in different concentrations of methanol (0, 0.5, 1.0, 1.5, and 2.0 mol/L) are presented in Fig.7b. When the concentration of methanol is low, almost no oxidation peak appears. As the concentration reaches 1.0 mol/L or higher, an oxidation peak at about 0.34 V can be observed obviously. The oxidation peak voltage is slightly increased while the concentration of methanol is aggrandized. Depending on the inset in Fig.7b, the oxidation peak current increases almost linearly as the concentration of methanol increases. In alkaline solution, the absorption of $OH^-$ and the formation of “gold pre-oxidation precursors” are important reasons for the catalysis of methanol oxidation on gold

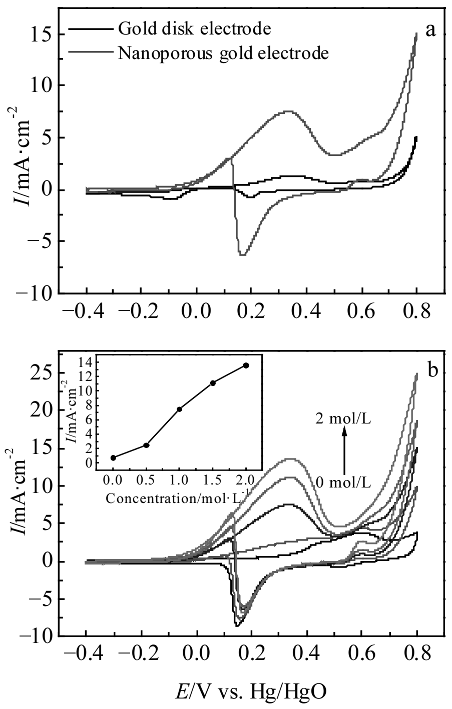

Fig.7 CV curves of prepared NPG electrode: (a) two kinds of electrodes in 1 mol/L methanol (the current density of gold disk electrode is amplified 5 times) and (b) NPG electrode in different concentrations of methanol (inset is the calibration plot of CV oxidation peak current versus concentration of methanol)

electrode[10]. The low-density and hierarchical nanoporous structure, produced by eliminating Ag and $SiO_2$, can provide a high surface area and a rapid mass transfer rate, resulting in larger adsorption capacity of $OH^-$ and active sites of pre-oxidation. Under these conditions, the adsorption of methanol on the surface of the gold electrode is the principal factor in controlling the oxidation reaction. Therefore, the oxidation peak current increases linearly with the increase of methanol concentration. Furthermore, with the increase of methanol concentration, the adsorption of methanol molecules is increased, while the adsorption of $OH^-$ is relatively reduced. This is why the oxidation peak voltage varies with the concentration of methanol. Because the overall adsorption capacity of $OH^-$ is relatively large, the oxidation peak voltage changes very little.

## 3 Conclusions

1) The combination of templating and dealloying technique is a novel way for synthesizing the hierarchical nanoporous Au foams with low-density and high surface area.

2) By continually changing corrosion solutions, the templates can be completely eliminated from $Au@Ag@SiO_2$ alloy and the Ag element can be dealloyed in corrosion solution. Prepared NPG foams are composed of large-sized hollows, spherical shells (~675 nm in diameter), and the small-sized ligament-pores (~75 nm). The ligament-pores are spread across the spherical shells.

3) The prepared low-density (1.1 $g/cm^3$, ~5.7% of relative density) and hierarchical NPG shows excellent catalytic activity and rapid mass transfer rate for methanol electro-oxidation in alkali solution, which implies a promising application in catalysis.

## References

1 Zeis R, Lei T, Sieradzki K. *Journal of Catalysis*[J], 2015, 253(1): 132

2 Gloria D, Gooding J J, Moran G. *Journal of Electroanalytical Chemistry*[J], 2011, 656(1-2): 114

3 Hartmann M. *Chem Mater*[J], 2005,17(18): 4577

4 Zhuang K, Wang L. *Nanosci Nanotech Let*[J], 2012, 4(4): 454

5 Zhuang L, Ma H, Sun H. *Biosensors & Bioelectronics*[J], 2017, 98: 29

6 Ding Y, Erlebache J. *J Am Chem Soc*[J], 2003, 125: 7772

7 Wittstock A, Zielasek V. *Science*[J], 2010, 327(5963): 319

8 Nagle L C, Rohan J F. *J Electrochem Soc*[J], 2011,158(7): 772

9 Yan X, Meng F, Xie Y *et al. Sci Rep*[J], 2012, 2: 941

10 Zhang J, Liu P, Houyi Ma A *et al. Journal of Physical Chemistry C*[J], 2007, 111(28): 10 382

11 Boonsa P, Kamsawat J. *Key Engineering Materials*[J], 2017, 728: 181

12 Huang J, Liu Y, He X. *RSC Advances*[J], 2017, 7(26): 15 747

13 Tan X, Wang J, Feng L *et al. Journal of Functional Materials*[J], 2017, 48(7): 7159

14 Dong C, Zhong M, Li L *et al. Sci Adv Mater*[J], 2012, 4(2): 204

15 Kong Q, Lian L, Liu Y *et al. Mater Lett*[J], 2014, 127: 59

16 Hakamada M, Kuromura T, Chino Y *et al. Mater Sci Eng A*[J], 2007, 459(1): 286

17 Jha N, Mondal D P, Dutta Majumdar J *et al. Mater Des*[J], 2013, 47(9): 810

18 Biener J, Nyce G W, Hodge A M *et al. Advanced Materials*[J], 2008, 20(6): 1211

19 Li Q, Lian L, Liu Y *et al. Advanced Engineering Materials*[J], 2017, 19(7): 1 700 045

20 Jiao L L, Sun J H. *Procedia Engineering*[J], 2014, 71: 622

21 Nyce G W, Hayes J R, Hamza A V *et al. Chemistry of Materials*[J], 2006, 19(3): 344

22 Stöber W, Fink A, Bohn E. *J Colloid Interface Sci*[J],1968, 26: 62

23 Wang A Q, Liu J H, Lin S D *et al. J Catal*[J], 2005, 233(1): 186

24 Sun Y, Balk T J. *Scripta Mater*[J], 2008, 58(9): 727

25 Kannan P, John S A. *Nanotechnology*[J], 2008, 19(8): 85 602

26 Thommes M. *Pure & Applied Chemistry*[J], 2015, 87: 1051

# 模板法-脱合金制备低密度分级纳米多孔金及其电催化性能

陈　静[1]，连利仙[1,2]，刘　颖[1,2]，汪　莉[1]

(1. 四川大学 材料科学与工程学院，四川 成都 610065)

(2. 四川大学 先进特种材料与技术教育部重点实验室，四川 成都 610065)

**摘　要**：提出了以模板法-脱合金复合方法制备低密度分级多孔金。以直径为 700 nm 的二氧化硅（$SiO_2$）微球作为模板，通过化学镀方法制备了 $Ag@SiO_2$ 和 $Au@Ag@SiO_2$ 核壳粒子，并通过冷压-烧结方法制备了 $Au@Ag@SiO_2$ 合金块材。通过连续改变腐蚀溶液，将 $SiO_2$ 模板以及 Ag 元素从 $Au@Ag@SiO_2$ 合金中完全去除。将 $SiO_2$ 从 $Au@Ag@SiO_2$ 微球完全去除从而得到了大尺寸空心球壳（直径约为 675 nm），将 Ag 元素脱合金去除从而在球壳表面形成了许多小尺寸的孔结构（直径约为 75 nm）。TEM 图像表明，块状金样品中的韧带由具有多晶特性的纳米晶粒组成。这种具有低密度 1.1 g/cm$^3$（相对密度为 5.7%）和高比表面积 4.24 m$^2$/g 的分级纳米多孔金材料在碱性溶液中对甲醇电氧化具有优良的催化活性以及快速的传质速率，表明其在催化领域具有广阔的应用前景。

**关键词**：纳米多孔金；模板法-脱合金化；分级的；低密度；电催化

---

作者简介：陈　静，男，1991 年生，硕士，四川大学材料科学与工程学院，四川 成都 610064，电话：028-85405332，E-mail: 18202851747@163.com